International Journal of Offshore and Coastal Engineering
Vol.10 | No. 1 | pp. 56 – 64 | May 2026
e-ISSN: 2580-0914

Submitted: November 22, 2025 | Revised: February 1, 2026 | Accepted: March 30, 2026

Analysis of Residual Fatigue Life on Jacket Platform Structure Due to Subsidence Effect

As Achmad Daffa Dhiya'udien Munaf[a,*], Nur Syahroni[a] and Handayanu[a]

[a)] Department of Ocean Engineering, Institut Teknologi Sepuluh Nopember, Surabaya, Indonesia
*Corresponding author: as.achmaddaffa@gmail.com

ABSTRACT

Many oil and gas platforms in Indonesian waters, both those still operating and those that have passed the operating life limit (expired), experience subsidence events, especially in the jacket platform structure. Subsidence around these platforms is caused by massive oil and gas exploitation in producing hydrocarbon reservoirs. This phenomenon poses a risk due to intolerable wave loads, where the waves increase the risk of structural failure, which can impact platform operations. Changes in seabed conditions due to subsidence will also affect the cyclical wave loads received by the platform jacket structure. In this Final Project, the author will analyze the residual fatigue life of the jacket platform structure due to subsidence. This Final Project research aims to analyze the effect of subsidence on the fatigue life of the jacket platform structure. Tests were carried out using cumulative damage and fracture mechanics methods to predict the failure time of the components reviewed in the jacket platform structure under non-subsidence conditions and when subsidence occurs. The analysis results show that the fatigue life of the structure will be reduced when subsidence occurs. With the cumulative damage method, the fatigue life value of the non-subsidence condition is 279 years, while the residual fatigue life of the structure in the subsidence condition is 59 years. Meanwhile, using the fracture mechanics method, the value of the fatigue life of the non-subsidence condition is 76 years, and the residual fatigue life of the structure in the subsidence condition is 41 years. These results show a significant decrease in the fatigue life of the structure.

Keywords: ***Jacket Platform, Fatigue, Subsidence, Cumulative Damage, Fracture Mechanics***

1. INTRODUCTION

Petroleum has become a necessity of life, with more than 85 million barrels of petroleum products consumed daily. To meet this huge demand for fossil fuels, petroleum companies are constantly searching for unexplored reserves on the earth. One of the most attractive sources is the ocean, which covers almost three-quarters of the earth's surface. Hence, these companies came up with the idea of constructing offshore structures to explore these precious treasures.

In Indonesian waters with an average water depth of less than 400 m, many offshore structures are used, namely fixed platform structures such as jacket platforms. Many oil and gas platforms operating or have passed the operating life limit (expired) experience subsidence events in Indonesian waters [1]. Subsidence around the platform occurs due to the massive exploitation of oil and gas in hydrocarbon reservoirs that are in production [2].

The subsidence that occurs on the platform will cause a reduction in the production period. If it has reached a certain stage of subsidence, the safety factor of the platform structure will be affected by the increase in MWL [3]. One of the significant effects of subsidence is to increase the overturning moment at the base of the jacket. This is because, in addition to the increasing wave force, the distance from the center of force to the mud line increases as subsidence increases [4]. Further subsidence rates will lead to intolerable risks and wave loads where waves occurring on the deck will cause a high level of increased risk of structural failure that can affect platform operations [3].

Fatigue failure in an offshore structure most often occurs when the structure is exposed to environmental loads, especially cyclical wave loads [5]. Changes in soil conditions due to subsidence will affect the cyclical wave loads received by the jacket platform structure. This research will analyze the residual fatigue life of the jacket platform structure due to subsidence.

2. THEORY

2.1 Subsidence

Subsidence is a decline that occurs globally in a land. This land subsidence is a process of land subsidence movement based on a certain datum [6]. Structural subsidence problems are mainly caused by subgrade deformation. The compressive deformation of soil is non-linear and unstable because the composition is very complex, and the soil will shift under a vertical load [7]. The effects of subsidence on the integrity of the jacket globally are as follows [8]:

a. movement of the piles concerning each other; b. high compressive forces within the lowermost jacket frame; c. rotation of the lowermost part of the jacket leg and consequent rotation of the pile sleeve cluster and the top of the pile; d. higher bending stresses in the pile due to the rotational effect of the top of the pile; e. more uneven distribution of the pile axial load within each pile group (push-pull effect within the pile group, resulting in increased pile axial design load); f. higher pile capacity and higher pile axial stiffness, due to higher soil friction generated between the pile surface and the surrounding soil; g. relatively larger upward vertical soil displacements and strains due to higher soil displacements and strains; and higher pile capacity and higher pile axial stiffness due to higher soil friction generated between the pile face and the surrounding soil; g. relatively larger upward vertical soil displacements and strains along the pile (equivalent to the Poisson effect) of about 60 mm.

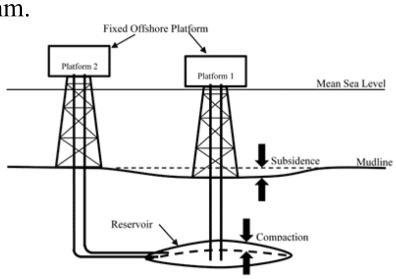

Figure 1. Illustration of subsidence in jacket platform [9]

2.2 In-place Analysis

The in-place analysis is used to examine platform structure failure modes when in-service. In-place analysis aims to ensure that the structure can withstand loads during operation, either gravity or environmental. The approach to in-place analysis is a static analysis approach, namely analysis when the structure is static or not affected by time under operating loading conditions (environmental loads with a return period of 1 year) and storms (environmental loads with a return period of 100 years). In the in-place analysis, it is necessary to consider UC ≤ 1 as the maximum allowable limit for the structure. Unity check (UC) is the ratio between the actual stress of the structure and the allowable stress with the following Equation 1.

$$\mathrm{UC} = \frac{\sigma_{act}}{\sigma_{all}} \quad (1)$$

2.3 Tubular Joint

The jacket structure consists of cylindrical or tubular members, which consist of two different types of members: main members (chord) and branch members (brace). The primary purpose of the tubular joint is to support the jacket in resisting lateral and vertical loads. The loads received by the jacket will be transferred to the tubular joint. At this tubular joint location, critical points occur along with repeated loading. Tubular joints are classified as K, X, and Y types based on their geometric arrangement.

According to API RP 2A-WSD 21st edition, tubular joints are arranged with the configuration and shape parameters, as shown in Figure 2 below.

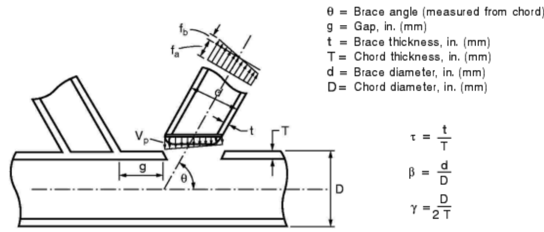

Figure 2. Tubular joint configuration parameters [10]

2.4 Fatigue Analysis

Fatigue analysis can be performed using two methods, deterministic and spectral. The deterministic method is used for structures that are not sensitive to dynamic forces, where all waves have a long period to reach the peak of the structure's transfer function. The sea state is discretized in relatively few discrete (deterministic) waves to determine the stress range values. The structure's response to these discrete waves is then calculated with or without dynamic effects. On the other hand, the spectral method uses a statistical approach to calculating fatigue damage in structures subjected to dynamic loading with many stress cycles. The spectral method uses wave spectra and transfer functions. Transfer function defines the ratio of cyclical stress range to wave height as a function of frequency. The following are the parameters used in fatigue analysis:

1) S-N Curve

The S-N curve represents the empirically determined relationship between stress range and number of failure cycles. S-N curves describe the characteristics of commonly used fatigue tests on materials subjected to repeated loading of the same magnitude.

2) Palmgren-Miner’s Rule

Fatigue failures are mainly caused by environmental loads, such as waves. The stresses caused by these loads are ever-changing and random in magnitude, so their amplitude varies. This rule allows fatigue damage to be calculated at several different load amplitudes. The fatigue concept is the basis of the Palmgren-Miner cumulative failure law, expressed in Equation 2 below.

$$D = \sum_{i=1}^{N} \frac{Napplied_i}{Nresisted_i} \quad (2)$$

Where,

D = the damage magnitude in 1 year
N = number of stress range group divisions
$Napplied_i$ = cycles in the working stress range
$Nresisted_i$ = cycles at the permissible stress range

3) Stress Concentration Factor (SCF)

SCF is the ratio between the highest stress at a position in the joint, namely hot-spot stress, and the nominal stress in the brace [11]. The value of the stress concentration factor is influenced by the geometry of the tubular joint, the type of tubular joint, and the loading type received. Accurately determining the stress concentration factor value is essential for predicting fatigue life. The following is Equation 3 to determine the SCF value.

$$SCF = \frac{\sigma_{hotspot}}{\sigma_{nominal}} \quad (3)$$

2.3 Hot-Spot Stress

Hot-spot stress is when a particular area or point on the structure experiences a significant increase in load or stress compared to other areas or points around it. This increase in load or stress can occur due to various factors, such as excessive loads, design errors, or load distribution imbalances. This hot-spot stress occurs at the weld toe location, considering the SCF caused by the discontinuity of the structure, which allows for cracking of the tubular joint.

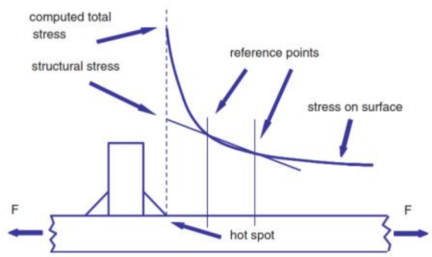

Figure 3. Hot-spot stress

2.4 Fracture Mechanics

Fracture mechanics is a method to analyze the fracture behavior of a structural joint by focusing on a specific area locally. This analysis is performed on tubular joints that will, are or have already experienced cracking. The fracture mechanics process involves several stages, such as crack initiation, crack propagation, and, eventually, a crack that can lead to structural failure (final fracture).

2.5 Stress Intensity Factor

The stress intensity factor (SIF) is one of the parameters that need to be considered in the crack failure approach using the fracture toughness method. The SIF value is also a parameter to predict the fatigue life of the structure. SIF is a function of stress, geometry, and crack size. The SIF value can be determined through the following Equation 4.

$$K = f_{(g)}\sigma_{nom}\sqrt{\pi a} \quad (4)$$

Where,
K = stress intensity factor (ksi√in)
a = initial crack depth
σ_{nom} = nominal stress
$f_{(g)}$ = correction function for dimension and crack geometry and position

2.6 Crack Propagation

Structural failure caused by cracking begins with the appearance of an initial crack. This stage marks the beginning of the failure process. The crack then propagates due to shear stress (microcrack growth stage) until it becomes a large crack affected by tensile stress (macro crack growth stage). This process continues until the component can no longer withstand the working stresses and finally breaks (final fracture). The Paris-Erdogan law in Equation 5 below can calculate the crack rate when propagation occurs.

$$\frac{da}{dN} = C(\Delta K^m) \quad (5)$$

Where,
da/dN = crack propagation rate (mm/cycle)
ΔK = stress intensity factor range
C and m = crack growth parameters

2.6 Fracture Mechanics - Fatigue Life Analysis

The fracture mechanics method's fatigue life is obtained by integrating the Paris-Erdogan law of crack propagation shown in Equation 6 below.

$$N = \int_{a_0}^{a_f} \frac{da}{C(\Delta K)^m} \quad (6)$$

where,
a_0 = initial crack depth
a_f = final crack depth
N = number of cycles
ΔK = SIF range
C and m = material constants

3. METHODOLOGY

3.1 Literature Review

This research begins with searching and studying references such as books, codes, previous Final Project reports from the Department of Ocean Engineering, and journals that have the same or similar topics. This process is carried out to support the theories used by the author in solving the problems discussed in this research.

3.2 General Data

The data required are jacket platform structure data, environmental data, loading data, and soil data on the jacket platform structure. Information about the data will be explained as follows.

Table 1. Environment data

Return Period	Wind Speed (mph)	Max Wave Height (ft)	Max Wave Period (sec)
1-year	38	18	7.3
100-year	63	32.4	9.8

Table 2. Platform data

Parameter	Description
Type	Wellhead Platform
Installation Year	1986
Number & Dimension Leg	4 (42” for jacket; 36” for deck)
Number & Dimension Pile	4 (36”)

Elevation	Jacket: EL. (+) 10' - 0" (Jacket Walkway) EL. (-) 22' - 0" EL. (-) 60' - 0" EL. (-) 96' - 0" (Mudmat Framing) Deck: EL. (+) 76' - 6" (Helideck) EL. (+) 58' - 6" (Main Deck) EL. (+) 38' - 0" (Cellar Deck) EL. (+) 29' - 6" (Wellhead Deck) EL. (+) 27' - 0" (Sub-Cellar Deck)

3.3 Platform Jacket Structure Model

The jacket platform structure is modeled according to the data obtained using SACS software. The structure is given loadings such as dead load, live load, equipment load, and environment load. To validate the model, the weight of the modeled jacket platform structure must be equalized with the weight of the original structure.

3.4 In-place Analysis

Perform an in-place analysis of the structure to get a unity check (UC) joint and member and determine the ability of the jacket platform structure to accept loads. The analysis is carried out in all directions to see which direction causes the structure to experience the most critical conditions before and after subsidence. This analysis is an approach to knowing the safe limit of the structure when subsidence occurs at each depth variation per one meter, validation with the condition that the UC value ≤ 1.

3.5 Fatigue Analysis – Cumulative Damage

Calculation of fatigue life using cumulative damage method assisted by SACS software. Calculations are carried out under both non-subsidence and subsidence conditions. The following are the steps in the cumulative damage method fatigue analysis:

1) Calculation of Natural Period for Non-Subsidence & Subsidence Condition
2) Wave Event Occurrence Input
3) Stress Concentration Factor (SCF) Calculation with SACS Software

3.6 Fatigue Analysis – Fracture Mechanics

Fatigue life is also calculated using the fracture mechanics method by modeling tubular joints with low fatigue life values and modeling cracks based on hot-spot stress with analysis using ANSYS software. The following are the stages in the fatigue analysis of the fracture mechanics method:

1) Determination of Critical Tubular Joint Location in Non-Subsidence & Subsidence Condition

Determining the critical tubular joint location is based on the results of the cumulative damage method fatigue analysis. The joint with the lowest fatigue life will be the critical local analysis joint.

2) Modeling and Input of Critical Tubular Joint Loading & Boundary Conditions

Critical tubular joint modeling is done with the help of ANSYS Workbench software. Loads and boundary conditions on the tubular joint are input according to the global analysis results. This is done to determine the location of the maximum stress reference point (hot-spot stress) on the tubular joint to be modeled as cracked.

3) Modeling of Semi-Elliptical Crack

Surface crack modeling with semi-elliptical type is carried out based on the maximum stress location, assuming that the crack depth value and crack length value are by the ABS: Guide for Fatigue Assessment of Offshore Structures.

4) Stress Intensity Factor (SIF) Calculation

Calculation of the SIF value is done using ANSYS after modelling the crack with the addition of crack length so that different SIF values are obtained. This SIF value is used to calculate the crack propagation rate, then validated with manual calculation.

5) Crack Propagation Calculation

The crack propagation rate is calculated manually using the Paris-Erdogan Law equation.

3.8 Fatigue Life Calculation

Calculate the fatigue life using a comparison of two methods, namely cumulative damage (global analysis) and fracture mechanics (local analysis), under non-subsidence and subsidence conditions.

4. RESULTS

4.1 Structure Modeling and Validation

The jacket platform structure is modelled using SACS software based on existing reference data. Next, the structural model was validated against the data in the platform report. The validation used is the Mean Absolute Percentage Error (MAPE) parameter with an error tolerance limit of 5%.

Table 3. Model Validation

Weight of Structure		Error (%)
Data	SACS	
3160.03	3107.85	1.65

Based on Table 3, the error value has met the tolerance limit of less than 5%. Thus, the structural model can be said to be valid and has presented the actual structure so that it can continue the next stage of analysis.

4.2 In-place Analysis

The inplace analysis was conducted for eight loading directions, including 0°, 45°, 90°, 135°, 180°, 225°, 270°, and 315°. In this in-place analysis, variations of subsidence occurrence under 100-years storm conditions with a depth of subsidence of one meter to four meters were performed. In this analysis, member stress checks were carried out in each loading direction and subsidence condition per meter. The analysis obtained shows that the most critical loading direction occurs in the 0° direction, with the UC value in each subsidence condition as follows.

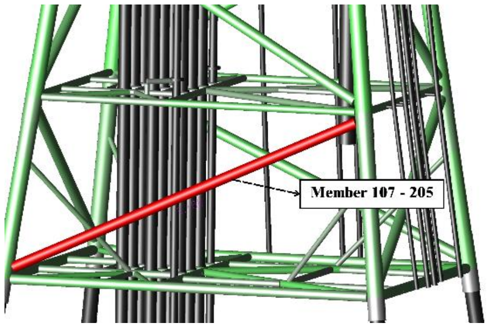

Figure 4. Critical Member

Table 4. Stress Check Member

Member	Max UC - Subsidence [-Z] (m)				
	0	1	2	3	4
107– 205	0.69	0.66	0.63	0.77	0.68

Table 4 shows that subsidence influences the UC member value; the UC value increases when the structure experiences subsidence events with a decrease in depth of three meters from the initial condition.

In the in-place analysis, a joint punching shear check was also carried out to determine the critical joint on the structure's jacket leg. The 12 tubular joints for each elevation of the jacket leg are reviewed under non-subsidence conditions, and the variations in subsidence per meter are as follows.

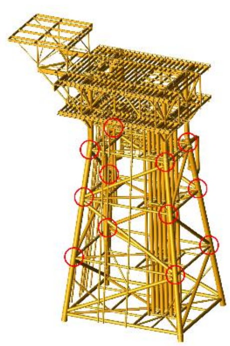

Figure 5. Reviewed Tubular Joint

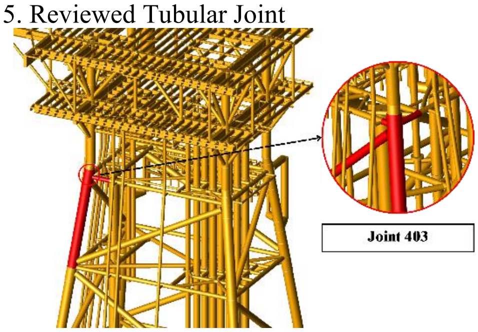

Figure 6. Critical Tubular Joint

Table 5. Joint Punching Shear Stress Check

Joint	Max UC - Subsidence [-Z] (m)				
	0	1	2	3	4
201	0.594	0.573	0.555	0.683	0.62
203	0.484	0.503	0.464	0.549	0.434
205	0.636	0.599	0.568	0.678	0.612
207	0.65	0.582	0.531	0.529	0.503
301	0.351	0.309	0.288	0.299	0.271
303	0.385	0.374	0.363	0.452	0.415
305	0.349	0.331	0.31	0.321	0.296
307	0.382	0.368	0.354	0.527	0.491
401	0.325	0.342	0.326	0.479	0.447
403	0.592	0.608	0.593	0.889	0.851
405	0.655	0.653	0.637	0.733	0.703
407	0.291	0.309	0.312	0.369	0.353

From Table 5, the critical joint occurring on the jacket leg is at joint 403 at EL (+) 10 ft, which is the connection between the jacket and the deck leg. The UC (Utilization Coefficient) of this joint increases when there is a subsidence of 3 meters. This is due to changes in environmental loads from waves and currents affecting the area between the topside and the jacket leg. The results of this joint punching shear check will form the basis for assuming the maximum subsidence depth.

4.2 Fatigue Analysis - Cumulative Damage Method

In analyzing fatigue using the cumulative damage method, the natural period value is first analyzed through dynamic structural analysis using the dynamic extract mode shape feature in the SACS software. This is done to determine whether the fatigue analysis will be performed using a deterministic or spectral approach. The following table presents the natural periods of the structure under both non-subsidence and subsidence conditions.

Table 6. Structure Natural Period

Non-Subsidence	Subsidence
1.71 seconds	1.69 seconds

Based on Table 6, since the period values are less than three seconds, the method used for the global fatigue analysis is deterministic fatigue. In the structural analysis, the structure is subjected to environmental loads, specifically cyclic wave loads, with the angle of attack as shown in Figure 9 below.

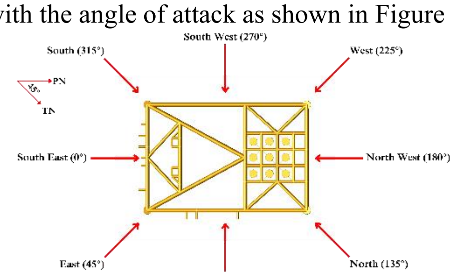

Figure 7. Wave Directions

In this study, fatigue life analysis is conducted by reviewing the main joints on the jacket structure as shown in the figure. The analysis is performed using the Palmgren-Miner hypothesis of linear cumulative damage and the appropriate S-N curve to predict fatigue life using the WJT curve as provided in the API RP 2A-WSD. The fatigue analysis is carried out with the help of SACS software to determine the fatigue life values for each tubular joint of the platform structure. The lowest fatigue life value is used to identify the critical tubular joint.

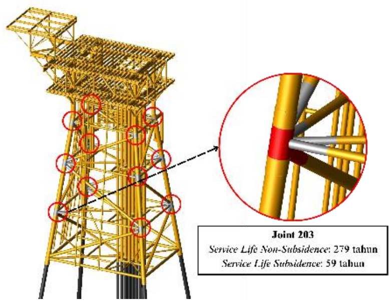

Figure 8. Tubular Joint with the Lowest Fatigue Life

From the analysis, it is found that the lowest fatigue life value is located at tubular joint 203. The author performed a geometric parameter validation for tubular joint 203 to ensure that the SCF values used to calculate the fatigue life are sufficiently accurate. Validation was conducted according to the parameters used for tubular joints based on the validity range parameters proposed by Efthymiou. The primary parameters, as shown in Figure 2, and the derived parameters include the diameter ratio (β= d/D), the thickness ratio (τ = t/T), the gap-to-diameter ratio (ζ = g/D), the chord slenderness ratio (γ = D/2T), the length-to-diameter ratio (α = 2L/D), and the angle between the chord and brace (θ).

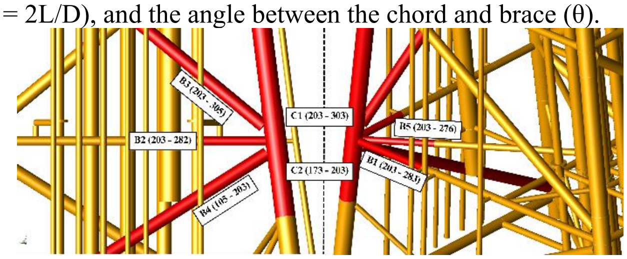

Figure 9. Tubular Joint 203

Below is the validation performed with the parameter ranges according to Efthymiou.

Parameter Utama

Parameter	Ukuran	Satuan	Parameter	Ukuran	Satuan
C1 & C2			C1 - B3 (KT Joint)		
			d_{B3}	26	in
$L_{C1 \& C2}$	126	in	t_{B3}	0.625	in
$D_{C1 \& C2}$	42	in	θ_{B3}	43.19	°
$T_{C1 \& C2}$	1.5	in	g_{B3-B2}	22.17	in
C1 - B1 (Y Joint)			C2 - B4 (KT Joint)		
d_{B1}	18	in	d_{B4}	26	in
t_{B1}	0.5	in	t_{B4}	1	in
θ_{B1}	89.93	°	θ_{B4}	64.60	°
g_{B1}	-	in	g_{B2-B4}	16.28	in
C1 - B2 (T Joint)			C1 - B5 (Y Joint)		
d_{B2}	18	in	d_{B5}	16	in
t_{B2}	0.5	in	t_{B5}	0.375	in
θ_{B2}	82.93	°	θ_{B5}	80.29	°
g_{B2}	-	in	g_{B5}	-	in

Parameter Turunan

Parameter		Nilai	Rentang Batas	Ket	Parameter		Nilai	Rentang Batas	Ket
β	β_{B1}	0.43	$0.2 \leq \beta \leq 1$	OK	γ	γ_{B1}	14	$10 \leq \gamma \leq 50$	OK
	β_{B2}	0.43		OK		γ_{B2}	14		OK
	β_{B3}	0.62		OK		γ_{B3}	14		OK
	β_{B4}	0.62		OK		γ_{B4}	14		OK
	β_{B5}	0.38		OK		γ_{B5}	14		OK
τ	τ_{B1}	0.33	$0.2 \leq \tau \leq 1$	OK	α	α_{B1}	6	$4 \leq \alpha \leq 40$	OK
	τ_{B2}	0.33		OK		α_{B2}	6		OK
	τ_{B3}	0.42		OK		α_{B3}	6		OK
	τ_{B4}	0.67		OK		α_{B4}	6		OK
	τ_{B5}	0.25		OK		α_{B5}	6		OK
ζ	ζ_{B1}	0	$-0.6 \leq \zeta$	OK	θ	θ_{B1}	89.93°	$30° \leq \theta \leq 90°$	OK
	ζ_{B2}	0		OK		θ_{B2}	82.93°		OK
	ζ_{B3}	0.53		OK		θ_{B3}	43.19°		OK
	ζ_{B4}	0.39		OK		θ_{B4}	64.6°		OK
	ζ_{B5}	0		OK		θ_{B5}	80.29°		OK

Figure 10. Tubular Joint Parameter Validations

It was found that the derived parameters of tubular joint 203 under review fall within the validity range parameters defined by Efthymiou, indicating that the calculated fatigue life values can be considered sufficiently accurate.

4.3 Fatigue Analysis - Fracture Mechanics Method

After conducting a global fatigue analysis (cumulative damage), a local fatigue analysis is also performed using the Linear Elastic Fracture Mechanics (LEFM) method. This method involves analyzing the fracture behaviour of a tubular joint with parameters including the SIF and crack propagation rate. By determining these two parameters, the fatigue life can be calculated.

Based on the results of the global analysis, the tubular joint with the lowest fatigue life (tubular joint 203), will be geometrically modelled using ANSYS software for further local analysis. Boundary conditions are applied to accurately represent the real conditions, with a fixed support in the chord member, and the analysis focuses on the connection between the chord and the brace. In addition to boundary conditions, loads are applied to each brace, including axial forces, in-plane bending (IPB), and out-of-plane bending (OPB).

Table 7. Loading on Tubular Joint

Member	Non-Subsidence			Subsidence		
	Axial (lbf)	IPB (lbf.in)	OPB (lbf.in)	Axial (lbf)	IPB (lbf.in)	OPB (lbf.in)
B1	-41534	43667	-39203	-47840	51568	-34444
B2	-26863	-41606	22573	-37578	-65533	42026
B3	122319	-252523	229113	154869	-359901	288721
B4	-138666	-737142	5898	-186077	-938884	-42534
B5	-5959	-33664	84953	-10349	-40651	140905

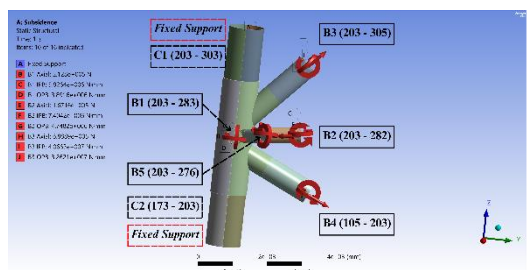

Figure 11. Local Analysis Model and Boundaries Condition

A mesh is applied to the model, and the sensitivity of the meshing is analyzed by reviewing stress probes at consistent locations to achieve accurate and stable stress distribution.

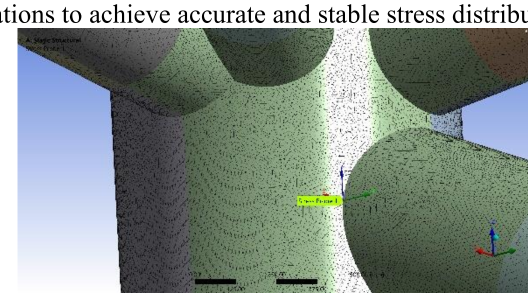

Figure 12. Model Mesh

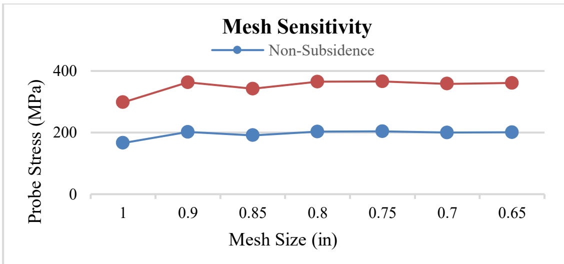

Figure 13. Mesh Sensitivity

From the graph, it is observed that the stress distribution becomes stable at a mesh size of 0.75 in. Therefore, this mesh size is used for further analysis.

In modeling the crack, the initial crack location is determined based on the maximum stress concentration (hot-spot stress). Maximum stress analysis is performed with the loads applied under both non-subsidence and subsidence conditions. The location of the maximum stress is found at the saddle brace connection between brace 4 and the chord.

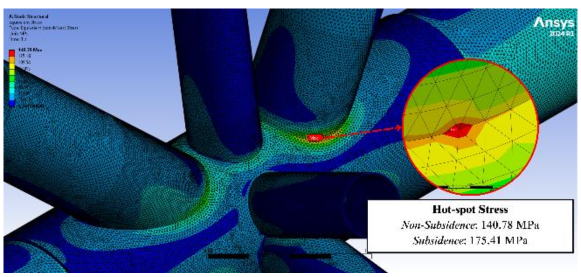

Figure 14. Maximum Stress

At the initial crack location, a surface crack will be modeled with a semi-elliptical shape. The assumed initial crack depth (a_0) is 0.5 mm [12]. With a crack depth-to-length ratio (a/2c) of 0.15 and 0.2, the crack length (2c) will be adjusted according to this ratio.

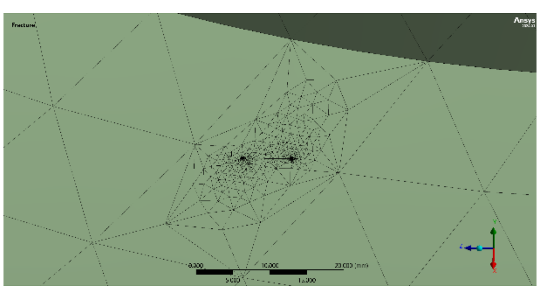
Figure 15. Crack Model

Crack modeling is performed from an initial crack depth (a_0) of 0.5 mm until it reaches the critical crack depth (a_{cr}) of 38.1 mm (1.5 in), which is equal to the wall thickness of the chord. The output of the crack modeling is the Stress Intensity Factor (SIF), is calculated with an incremental crack growth of 0.5 mm from the initial crack to the final crack depth. In this study, the crack analysis mode used is Mode I with example analysis results provided as follows.

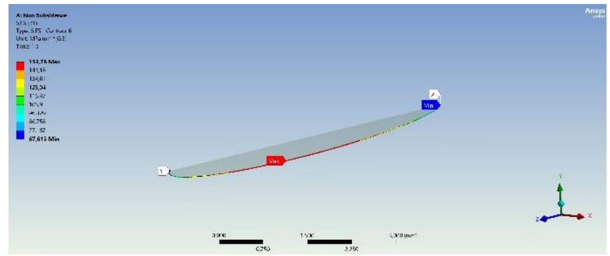
Figure 16. SIF Analysis Result

The numerically obtained SIF values are then validated manually by using Equation 7 for surface crack as follows.

$$K_I = 1.12\sigma\sqrt{\pi\frac{a}{Q}M_K} \quad (7)$$

where the value of Mk (back free surface correction factor) can be determined using Equation 8 as follows.

$$M_K = 1.0 + 1.2\left(\frac{a}{t} - 0.5\right) \quad (8)$$

where the value of Q (front free surface correction factor) can be determined using Equation 9 as follows [13]:

$$Q = 1 + 1.464\left(\frac{a}{c}\right)^{1.65} \quad (9)$$

With the maximum stress at the initial crack location being 115.57 MPa (non-subsidence) and 152.01 MPa (subsidence), the SIF values can be calculated and validated as shown in the following table.

Table 8. SIF Values

Condition	Crack Ratio (a/2c)	SIF (MPa√mm) Manual	SIF (MPa√mm) ANSYS	Error (%)
Non-Subsidence	0.15	148.09	153.76	3.82
	0.2	141.05	149.01	5.65
Subsidence	0.15	194.79	186.94	4.03
	0.2	185.52	183.44	1.13

Since the error is less than 10%, the SIF values can be considered valid. The fatigue life of the structure can be determined by the crack propagation rate. The crack propagation rate for ASTM A36 steel can be calculated using Equation 10 as follows.

$$\frac{da}{dN} = 3.6 \times 10^{-10}(\Delta K_I)^{3.0} \quad (10)$$

From the crack propagation rate, the fatigue life can be calculated by determining the number of cycles until failure as described by Equation 6. The number of cycles experienced is shown as follows.

Non-Subsidence

a (mm)	a (in)	a_f (in)	a_{avg} (in)	Rasio Retak (a/2c = 0.15) ΔK (ksi√in)	da/dN (in/cycle)	ΔN (cycles)	Rasio Retak (a/2c = 0.2) ΔK (ksi√in)	da/dN (in/cycle)	ΔN (cycles)
0	0.00	0.02	0.01	2.48	5.48.E-09	9.12.E+07	2.18	3.73.E-09	1.34.E+08
0.50	0.02	0.04	0.03	3.41	1.43.E-08	3.50.E+07	2.93	9.08.E-09	5.50.E+07
1.00	0.04	0.06	0.05	4.07	2.43.E-08	2.05.E+07	3.48	1.51.E-08	3.30.E+07
1.50	0.06	0.08	0.07	4.71	3.76.E-08	1.33.E+07	3.95	2.22.E-08	2.25.E+07
2.00	0.08	0.10	0.09	5.20	5.05.E-08	9.89.E+06	4.38	3.02.E-08	1.66.E+07
2.50	0.10	0.12	0.11	5.63	6.42.E-08	7.78.E+06	4.73	3.82.E-08	1.31.E+07
3.00	0.12	0.14	0.13	5.94	7.56.E-08	6.62.E+06	5.05	4.64.E-08	1.08.E+07
3.50	0.14	0.16	0.15	6.39	9.38.E-08	5.33.E+06	5.34	5.47.E-08	9.14.E+06
4.00	0.16	0.18	0.17	6.70	1.08.E-07	4.61.E+06	5.59	6.30.E-08	7.94.E+06
4.50	0.18	0.20	0.19	7.00	1.23.E-07	4.05.E+06	5.81	7.07.E-08	7.07.E+06
5.00	0.20	0.22	0.21	7.32	1.41.E-07	3.54.E+06	6.01	7.80.E-08	6.41.E+06
5.50	0.22	0.24	0.23	7.30	1.40.E-07	3.57.E+06	6.22	8.67.E-08	5.77.E+06
6.00	0.24	0.26	0.25	7.86	1.75.E-07	2.86.E+06	6.40	9.43.E-08	5.30.E+06
6.50	0.26	0.28	0.27	8.07	1.89.E-07	2.65.E+06	6.53	1.00.E-07	4.98.E+06
7.00	0.28	0.30	0.29	8.29	2.05.E-07	2.44.E+06	6.69	1.08.E-07	4.64.E+06
7.50	0.30	0.31	0.31	8.51	2.22.E-07	2.26.E+06	6.79	1.13.E-07	4.43.E+06
8.00	0.31	0.33	0.32	8.65	2.33.E-07	2.15.E+06	6.89	1.18.E-07	4.24.E+06
8.50	0.33	0.35	0.34	8.89	2.53.E-07	1.98.E+06	7.02	1.25.E-07	4.01.E+06
9.00	0.35	0.37	0.36	9.04	2.66.E-07	1.88.E+06	7.02	1.25.E-07	4.01.E+06
9.50	0.37	0.39	0.38	9.23	2.83.E-07	1.77.E+06	7.13	1.30.E-07	3.83.E+06
10.00	0.39	0.41	0.40	9.42	3.01.E-07	1.66.E+06	7.11	1.29.E-07	3.86.E+06
10.50	0.41	0.43	0.42	9.49	3.07.E-07	1.63.E+06	7.19	1.34.E-07	3.73.E+06
11.00	0.43	0.45	0.44	9.70	3.28.E-07	1.52.E+06	7.20	1.34.E-07	3.72.E+06
11.50	0.45	0.47	0.46	9.76	3.34.E-07	1.50.E+06	7.26	1.38.E-07	3.64.E+06
12.00	0.47	0.49	0.48	9.87	3.46.E-07	1.45.E+06	7.24	1.36.E-07	3.66.E+06
12.50	0.49	0.51	0.50	9.71	3.30.E-07	1.52.E+06	7.20	1.34.E-07	3.72.E+06
13.00	0.51	0.53	0.52	9.95	3.55.E-07	1.41.E+06	7.27	1.38.E-07	3.62.E+06
13.50	0.53	0.55	0.54	10.21	3.84.E-07	1.30.E+06	7.24	1.37.E-07	3.66.E+06
14.00	0.55	0.57	0.56	10.25	3.88.E-07	1.29.E+06	7.24	1.37.E-07	3.66.E+06
14.50	0.57	0.59	0.58	10.35	3.99.E-07	1.25.E+06	7.22	1.35.E-07	3.69.E+06
15.00	0.59	0.61	0.60	10.39	4.04.E-07	1.24.E+06	7.24	1.36.E-07	3.66.E+06
15.50	0.61	0.63	0.62	10.46	4.12.E-07	1.21.E+06	6.99	1.23.E-07	4.07.E+06
16.00	0.63	0.65	0.64	10.54	4.21.E-07	1.19.E+06	7.19	1.34.E-07	3.73.E+06
16.50	0.65	0.67	0.66	10.36	4.01.E-07	1.25.E+06	7.16	1.32.E-07	3.78.E+06
17.00	0.67	0.69	0.68	10.65	4.35.E-07	1.15.E+06	7.15	1.31.E-07	3.80.E+06
17.50	0.69	0.71	0.70	10.70	4.41.E-07	1.13.E+06	7.23	1.36.E-07	3.68.E+06
18.00	0.71	0.73	0.72	10.73	4.45.E-07	1.12.E+06	7.23	1.36.E-07	3.67.E+06
18.50	0.73	0.75	0.74	10.80	4.53.E-07	1.10.E+06	7.18	1.33.E-07	3.75.E+06
19.00	0.75	0.77	0.76	10.64	4.34.E-07	1.15.E+06	7.22	1.35.E-07	3.69.E+06

Non-Subsidence

a (mm)	a (in)	a_f (in)	a_{avg} (in)	Rasio Retak (a/2c = 0.15) ΔK (ksi√in)	da/dN (in/cycle)	ΔN (cycles)	Rasio Retak (a/2c = 0.2) ΔK (ksi√in)	da/dN (in/cycle)	ΔN (cycles)
19.50	0.77	0.79	0.78	10.82	4.56.E-07	1.10.E+06	7.22	1.36.E-07	3.68.E+06
20.00	0.79	0.81	0.80	10.77	4.50.E-07	1.11.E+06	7.23	1.36.E-07	3.67.E+06
20.50	0.81	0.83	0.82	10.81	4.54.E-07	1.10.E+06	7.26	1.38.E-07	3.63.E+06
21.00	0.83	0.85	0.84	10.80	4.53.E-07	1.10.E+06	7.05	1.26.E-07	3.97.E+06
21.50	0.85	0.87	0.86	11.00	4.80.E-07	1.04.E+06	7.08	1.28.E-07	3.91.E+06
22.00	0.87	0.89	0.88	10.96	4.74.E-07	1.05.E+06	7.11	1.29.E-07	3.86.E+06
22.50	0.89	0.91	0.90	11.04	4.84.E-07	1.03.E+06	7.36	1.43.E-07	3.48.E+06
23.00	0.91	0.93	0.92	11.07	4.89.E-07	1.02.E+06	7.01	1.24.E-07	4.03.E+06
23.50	0.93	0.94	0.94	10.58	4.27.E-07	1.17.E+06	7.38	1.45.E-07	3.46.E+06
24.00	0.94	0.96	0.95	10.41	4.06.E-07	1.23.E+06	7.37	1.44.E-07	3.47.E+06
24.50	0.96	0.98	0.97	10.56	4.24.E-07	1.18.E+06	7.44	1.48.E-07	3.37.E+06
25.00	0.98	1.00	0.99	11.33	5.23.E-07	9.56.E+05	7.46	1.49.E-07	3.35.E+06
25.50	1.00	1.02	1.01	10.00	3.60.E-07	1.39.E+06	7.44	1.48.E-07	3.37.E+06
26.00	1.02	1.04	1.03	11.34	5.25.E-07	9.52.E+05	7.47	1.50.E-07	3.34.E+06
26.50	1.04	1.06	1.05	11.35	5.26.E-07	9.50.E+05	7.32	1.41.E-07	3.54.E+06
27.00	1.06	1.08	1.07	11.51	5.49.E-07	9.11.E+05	7.49	1.51.E-07	3.31.E+06
27.50	1.08	1.10	1.09	11.55	5.54.E-07	9.02.E+05	7.54	1.55.E-07	3.23.E+06
28.00	1.10	1.12	1.11	11.60	5.62.E-07	8.89.E+05	7.49	1.51.E-07	3.31.E+06
28.50	1.12	1.14	1.13	11.49	5.47.E-07	9.15.E+05	7.50	1.52.E-07	3.30.E+06
29.00	1.14	1.16	1.15	11.66	5.71.E-07	8.75.E+05	7.48	1.51.E-07	3.32.E+06
29.50	1.16	1.18	1.17	11.59	5.60.E-07	8.93.E+05	7.54	1.55.E-07	3.24.E+06
30.00	1.18	1.20	1.19	11.59	5.61.E-07	8.92.E+05	7.74	1.67.E-07	2.99.E+06
30.50	1.20	1.22	1.21	11.58	5.60.E-07	8.93.E+05	8.48	2.19.E-07	2.28.E+06
31.00	1.22	1.24	1.23	11.60	5.62.E-07	8.89.E+05	10.18	3.80.E-07	1.32.E+06
31.50	1.24	1.26	1.25	11.62	5.64.E-07	8.86.E+05	9.84	3.43.E-07	1.46.E+06
32.00	1.26	1.28	1.27	11.25	5.12.E-07	9.77.E+05	10.40	4.05.E-07	1.23.E+06
32.50	1.28	1.30	1.29	11.69	5.75.E-07	8.70.E+05	11.38	5.31.E-07	9.42.E+05
33.00	1.30	1.32	1.31	11.62	5.64.E-07	8.86.E+05	12.21	6.55.E-07	7.63.E+05
33.50	1.32	1.34	1.33	11.62	5.65.E-07	8.85.E+05	13.34	8.55.E-07	5.85.E+05
34.00	1.34	1.36	1.35	11.77	5.86.E-07	8.53.E+05	13.99	9.86.E-07	5.07.E+05
34.50	1.36	1.38	1.37	14.93	1.20.E-06	4.17.E+05	15.20	1.26.E-06	3.96.E+05
35.00	1.38	1.40	1.39	13.77	9.40.E-07	5.32.E+05	16.70	1.68.E-06	2.98.E+05
35.50	1.40	1.42	1.41	16.32	1.56.E-06	3.20.E+05	17.47	1.92.E-06	2.61.E+05
36.00	1.42	1.44	1.43	16.48	1.61.E-06	3.11.E+05	18.35	2.23.E-06	2.25.E+05
36.50	1.44	1.46	1.45	16.85	1.72.E-06	2.90.E+05	19.28	2.58.E-06	1.94.E+05
37.00	1.46	1.48	1.47	16.35	1.57.E-06	3.18.E+05	19.46	2.65.E-06	1.88.E+05
					N	**2.80.E+08**		N	**5.15.E+08**

Figure 17. Number of Cycles for Non-Subsidence Condition

Subsidence

a (mm)	a (in)	a_f (in)	a_{avg} (in)	Rasio Retak (a/2c = 0.15) ΔK (ksi√in)	da/dN (in/cycle)	ΔN (cycles)	Rasio Retak (a/2c = 0.2) ΔK (ksi√in)	da/dN (in/cycle)	ΔN (cycles)
0	0.00	0.02	0.01	3.08	1.06.E-08	4.73.E+07	2.61	6.37.E-09	7.85.E+07
0.50	0.02	0.04	0.03	4.16	2.59.E-08	1.93.E+07	3.63	1.73.E-08	2.90.E+07
1.00	0.04	0.06	0.05	4.98	4.46.E-08	1.12.E+07	4.30	2.87.E-08	1.74.E+07
1.50	0.06	0.08	0.07	5.76	6.87.E-08	7.28.E+06	4.88	4.17.E-08	1.20.E+07
2.00	0.08	0.10	0.09	6.37	9.32.E-08	5.36.E+06	5.43	5.76.E-08	8.68.E+06
2.50	0.10	0.12	0.11	6.96	1.21.E-07	4.12.E+06	5.85	7.19.E-08	6.95.E+06
3.00	0.12	0.14	0.13	7.43	1.48.E-07	3.39.E+06	6.25	8.80.E-08	5.68.E+06
3.50	0.14	0.16	0.15	7.91	1.78.E-07	2.81.E+06	6.58	1.03.E-07	4.87.E+06
4.00	0.16	0.18	0.17	8.33	2.08.E-07	2.40.E+06	6.90	1.18.E-07	4.22.E+06
4.50	0.18	0.20	0.19	8.71	2.38.E-07	2.10.E+06	7.21	1.35.E-07	3.70.E+06
5.00	0.20	0.22	0.21	9.08	2.70.E-07	1.85.E+06	7.47	1.50.E-07	3.33.E+06
5.50	0.22	0.24	0.23	9.43	3.02.E-07	1.66.E+06	7.69	1.64.E-07	3.05.E+06
6.00	0.24	0.26	0.25	9.74	3.32.E-07	1.51.E+06	7.89	1.77.E-07	2.83.E+06
6.50	0.26	0.28	0.27	10.06	3.67.E-07	1.36.E+06	8.01	1.85.E-07	2.70.E+06
7.00	0.28	0.30	0.29	10.33	3.97.E-07	1.26.E+06	8.28	2.04.E-07	2.45.E+06
7.50	0.30	0.31	0.31	10.54	4.22.E-07	1.18.E+06	8.39	2.13.E-07	2.35.E+06
8.00	0.31	0.33	0.32	10.76	4.48.E-07	1.12.E+06	8.54	2.24.E-07	2.23.E+06
8.50	0.33	0.35	0.34	11.05	4.85.E-07	1.03.E+06	8.62	2.31.E-07	2.17.E+06
9.00	0.35	0.37	0.36	11.25	5.13.E-07	9.75.E+05	8.70	2.37.E-07	2.11.E+06
9.50	0.37	0.39	0.38	11.44	5.39.E-07	9.28.E+05	8.84	2.49.E-07	2.01.E+06
10.00	0.39	0.41	0.40	11.61	5.63.E-07	8.88.E+05	8.90	2.53.E-07	1.97.E+06
10.50	0.41	0.43	0.42	11.80	5.92.E-07	8.45.E+05	8.94	2.58.E-07	1.94.E+06
11.00	0.43	0.45	0.44	12.03	6.26.E-07	7.99.E+05	8.99	2.62.E-07	1.91.E+06
11.50	0.45	0.47	0.46	12.12	6.41.E-07	7.80.E+05	9.02	2.64.E-07	1.89.E+06
12.00	0.47	0.49	0.48	12.29	6.68.E-07	7.48.E+05	9.14	2.75.E-07	1.82.E+06
12.50	0.49	0.51	0.50	12.42	6.90.E-07	7.24.E+05	9.05	2.67.E-07	1.87.E+06
13.00	0.51	0.53	0.52	12.55	7.11.E-07	7.03.E+05	9.04	2.66.E-07	1.88.E+06
13.50	0.53	0.55	0.54	12.68	7.33.E-07	6.82.E+05	9.01	2.64.E-07	1.90.E+06
14.00	0.55	0.57	0.56	12.84	7.62.E-07	6.56.E+05	8.98	2.60.E-07	1.92.E+06
14.50	0.57	0.59	0.58	12.92	7.77.E-07	6.44.E+05	9.03	2.65.E-07	1.89.E+06
15.00	0.59	0.61	0.60	13.00	7.92.E-07	6.32.E+05	8.95	2.58.E-07	1.94.E+06
15.50	0.61	0.63	0.62	13.11	8.12.E-07	6.16.E+05	9.00	2.63.E-07	1.90.E+06
16.00	0.63	0.65	0.64	13.13	8.14.E-07	6.14.E+05	8.99	2.61.E-07	1.91.E+06
16.50	0.65	0.67	0.66	13.19	8.26.E-07	6.06.E+05	8.98	2.61.E-07	1.92.E+06
17.00	0.67	0.69	0.68	13.35	8.57.E-07	5.83.E+05	8.95	2.58.E-07	1.94.E+06
17.50	0.69	0.71	0.70	13.46	8.79.E-07	5.69.E+05	8.99	2.62.E-07	1.91.E+06
18.00	0.71	0.73	0.72	13.52	8.89.E-07	5.62.E+05	8.94	2.57.E-07	1.95.E+06
18.50	0.73	0.75	0.74	13.52	8.90.E-07	5.62.E+05	8.94	2.57.E-07	1.94.E+06
19.00	0.75	0.77	0.76	13.62	9.10.E-07	5.49.E+05	9.01	2.63.E-07	1.90.E+06

Subsidence

a (mm)	a (in)	a_f (in)	a_{avg} (in)	Rasio Retak (a/2c = 0.15) ΔK (ksi√in)	da/dN (in/cycle)	ΔN (cycles)	Rasio Retak (a/2c = 0.2) ΔK (ksi√in)	da/dN (in/cycle)	ΔN (cycles)
19.00	0.75	0.77	0.76	13.62	9.10.E-07	5.49.E+05	9.01	2.63.E-07	1.90.E+06
19.50	0.77	0.79	0.78	13.58	9.02.E-07	5.55.E+05	8.98	2.61.E-07	1.92.E+06
20.00	0.79	0.81	0.80	13.58	9.01.E-07	5.55.E+05	8.98	2.61.E-07	1.92.E+06
20.50	0.81	0.83	0.82	13.72	9.29.E-07	5.38.E+05	9.02	2.64.E-07	1.89.E+06
21.00	0.83	0.85	0.84	13.60	9.05.E-07	5.53.E+05	8.76	2.42.E-07	2.07.E+06
21.50	0.85	0.87	0.86	13.68	9.22.E-07	5.42.E+05	9.08	2.69.E-07	1.86.E+06
22.00	0.87	0.89	0.88	13.76	9.39.E-07	5.33.E+05	8.84	2.48.E-07	2.01.E+06
22.50	0.89	0.91	0.90	13.74	9.33.E-07	5.36.E+05	9.15	2.76.E-07	1.81.E+06
23.00	0.91	0.93	0.92	13.37	8.60.E-07	5.81.E+05	8.72	2.39.E-07	2.09.E+06
23.50	0.93	0.94	0.94	13.93	9.74.E-07	5.14.E+05	9.18	2.78.E-07	1.80.E+06
24.00	0.94	0.96	0.95	13.96	9.80.E-07	5.10.E+05	9.18	2.78.E-07	1.80.E+06
24.50	0.96	0.98	0.97	14.07	1.00.E-06	4.99.E+05	9.27	2.87.E-07	1.74.E+06
25.00	0.98	1.00	0.99	14.10	1.01.E-06	4.96.E+05	9.30	2.89.E-07	1.73.E+06
25.50	1.00	1.02	1.01	14.17	1.02.E-06	4.89.E+05	9.27	2.87.E-07	1.74.E+06
26.00	1.02	1.04	1.03	14.31	1.05.E-06	4.74.E+05	9.32	2.91.E-07	1.72.E+06
26.50	1.04	1.06	1.05	14.32	1.06.E-06	4.73.E+05	9.13	2.74.E-07	1.82.E+06
27.00	1.06	1.08	1.07	14.45	1.09.E-06	4.60.E+05	9.34	2.94.E-07	1.70.E+06
27.50	1.08	1.10	1.09	14.46	1.09.E-06	4.59.E+05	9.42	3.01.E-07	1.66.E+06
28.00	1.10	1.12	1.11	14.28	1.05.E-06	4.77.E+05	9.35	2.94.E-07	1.70.E+06
28.50	1.12	1.14	1.13	14.45	1.09.E-06	4.60.E+05	9.36	2.95.E-07	1.69.E+06
29.00	1.14	1.16	1.15	14.57	1.11.E-06	4.49.E+05	9.34	2.93.E-07	1.71.E+06
29.50	1.16	1.18	1.17	14.58	1.11.E-06	4.48.E+05	9.44	3.02.E-07	1.65.E+06
30.00	1.18	1.20	1.19	14.59	1.12.E-06	4.47.E+05	9.38	2.97.E-07	1.68.E+06
30.50	1.20	1.22	1.21	14.77	1.16.E-06	4.31.E+05	10.23	3.86.E-07	1.30.E+06
31.00	1.22	1.24	1.23	14.67	1.14.E-06	4.40.E+05	12.32	6.73.E-07	7.43.E+05
31.50	1.24	1.26	1.25	14.72	1.15.E-06	4.36.E+05	11.90	6.07.E-07	8.24.E+05
32.00	1.26	1.28	1.27	13.72	9.29.E-07	5.38.E+05	12.60	7.20.E-07	6.94.E+05
32.50	1.28	1.30	1.29	13.61	9.07.E-07	5.51.E+05	13.81	9.47.E-07	5.28.E+05
33.00	1.30	1.32	1.31	14.73	1.15.E-06	4.35.E+05	14.80	1.17.E-06	4.28.E+05
33.50	1.32	1.34	1.33	14.70	1.14.E-06	4.37.E+05	16.20	1.53.E-06	3.27.E+05
34.00	1.34	1.36	1.35	14.75	1.15.E-06	4.33.E+05	17.00	1.77.E-06	2.83.E+05
34.50	1.36	1.38	1.37	16.62	1.65.E-06	3.03.E+05	18.45	2.26.E-06	2.21.E+05
35.00	1.38	1.40	1.39	16.94	1.75.E-06	2.86.E+05	20.28	3.00.E-06	1.67.E+05
35.50	1.40	1.42	1.41	18.36	2.23.E-06	2.24.E+05	21.65	3.66.E-06	1.37.E+05
36.00	1.42	1.44	1.43	19.07	2.50.E-06	2.00.E+05	21.36	3.51.E-06	1.42.E+05
36.50	1.44	1.46	1.45	20.14	2.94.E-06	1.70.E+05	24.37	5.21.E-06	9.59.E+04
37.00	1.46	1.48	1.47	21.34	3.50.E-06	1.43.E+05	23.92	4.93.E-06	1.01.E+05
					N	**1.47.E+08**		N	**2.78.E+08**

Figure 18. Number of Cycles for Subsidence Condition

The results of the fatigue life for the structure under non-subsidence and subsidence conditions can be seen in the following table.

Table 9. Fatigue Life Using Fracture Mechanics Method

Condition	Description	Value a/2c = 0.15	Value a/2c = 0.2
Non-Subsidence	Cycle Number	280471701	514961030
	Number of Waves	6750000	6750000
	Fatigue Life (years)	42	76
Subsidence	Cycle Number	146968082	278228655
	Number of Waves	6750000	6750000
	Fatigue Life (Years)	22	41

Table 10. Fatigue Life Comparation

Condition	Fatigue Life (Years) Cumulative Damage	Fracture Mechanics a/2c = 0.15	Fracture Mechanics a/2c = 0.2
Non-Subsidence	279	42	76
Subsidence	59	22	41

From Table 10, it is observed that the fatigue life significantly decreases when subsidence events occur on the jacket platform. The effect of the crack ratio on the obtained fatigue life shows that as the crack ratio increases, the fatigue life also increases.

5. CONCLUSIONS

From the analysis and discussion conducted, it can be concluded that the unity check (UC) values increase with subsidence at a depth of three meters. The critical member is identified as the jacket vertical bracing, which has a UC value of 0.77, while the most critical tubular joint is at the connection between the jacket and the deck leg, with a UC value of 0.889. This increase is attributed to changes in environmental loads caused by waves and currents impacting the area between the topside and the jacket leg due to subsidence.

The critical tubular joint identified is joint 203 based on cumulative damage fatigue analysis, with a fatigue life of 279 years (non-subsidence) and a residual fatigue life is 59 years (subsidence). Additionally, fracture mechanics fatigue analysis shows a fatigue life of 42 years (a/2c=0.15) and 76 years (a/2c=0.2) under non-subsidence conditions. Under subsidence, the residual fatigue life is 22 years (a/2c=0.15) and 41 years (a/2c=0.15). These findings indicate a significant decrease in the structure's fatigue life in the event of subsidence. All references cited in the text are listed sequentially in the reference list at the end of the paper.

REFERENCES

[1] API, API RP 2A-WSD: Recommended Practice for Planning, Designing, and Constructing Fixed Offshore Platforms — Working Stress Design, 21st ed. Washington: American Petroleum Institute, 2000.

[2] API, API RP 2A-WSD: Planning, Designing, and Constructing Fixed Offshore Platforms — Working Stress Design, 22nd ed., no. November. Washington: American Petroleum Institute, 2014.

[3] ABS, "Guide for Fatigue Assessment Of Offshore Structures 2020," no. June, 2020.

[4] J. C. Newman and I. S. Raju, "An empirical stress-intensity factor equation for the surface crack," Eng. Fract. Mech., vol. 15, no. 1, pp. 185–192, 1981, doi: https://doi.org/10.1016/0013-7944(81)90116-8.

[5] A. Jha, O. Kiciman, J. Gebara, B. Stahl, and K. Dahl-Stamnes, "Assessment of Offshore Platforms Under Subsidence - Part II: Analysis and Results," J. Offshore Mech. Arct. Eng., vol. 122, no. 4, pp. 267–273, 2000, doi: 10.1115/1.1313531.

[6] N. U. Azman, M. K. Abu Husain, N. I. Mohd Zaki, E. Mat Soom, A. Mukhlas, and S. Z. A. Syed Ahmad, "Structural Integrity of Fixed Offshore Platforms by Incorporating Wave-in-Deck," J. Mar. Sci. Eng., vol. 9, p. 1027, Sep. 2021, doi: 10.3390/jmse9091027.

[7] W. Yanlin, B. Xiangjun, F. Sheng, M. Yingxin, and Y. Qianjin, "Subsidence Monitoring of Offshore Platforms," Procedia Eng., vol. 15, pp. 1015–1020, 2011,doi:https://doi.org/10.1016/j.proeng.2011.08.188

[8] A. Rafiudin and H. Firmansyah, "Analisis Linier dan Non Linier Struktur Anjungan Lepas Pantai Akibat Subsidence," Institut Teknologi Bandung, 2008.

[Online]. Available: https://digilib.itb.ac.id/gdl/view/7118/subsidence?rows=6&per_page=3&fid=7
[9] P. Broughton, "The Effects of Subsidence on the Steel Jacket and Piled Foundation Designs for the Ekofisk 2/4X and 2/4J Platforms," Proc. Inst. Civ. Eng. Water Marit. Eng., vol. 118, no. 2, pp. 88–102, 1996, doi: 10.1680/iwtme.1996.28430.
[10] S. Rismarini, "ANALISIS UMUR KELELAHAN KONTRUKSI YOKE ARM PADA EKSTERNAL TURRET MOORING SYSTEM FSO LADINDA," 2016.
[11] A. Aulia, "Analisis Risiko Keruntuhan Jacket Wellhead Tripod Platform Pasca Subsidence," Institut Teknologi Sepuluh Nopember, 2023.
[12] B. B. Kumoro, "Analisa Pengaruh Subsidence Terhadap Integritas Struktur Jacket Platform," Institut Teknologi Sepuluh Nopember, 2005.
[13] S. Ainnillah, "Analisa Ultimate Strength Struktur Jacket Platform Berbasis Keandalan Pasca Subsidence," Institut Teknologi Sepuluh Nopember, 2017.